

Gapped Energy Spectra around the Dirac Node at the Surface of a Three-Dimensional Topological Insulator in the Presence of the Time-Reversal Symmetry

Tetsuro HABA^{1*} and Yasuhiro ASANO^{1,2}

¹Department of Applied Physics, Hokkaido University, Sapporo 060-8628, Japan

²Center for Topological Science and Technology, Hokkaido University, Sapporo 060-8628, Japan

(Received February 19, 2013; accepted April 5, 2013; published online May 7, 2013)

We discuss the excitation spectra around the Dirac node on a surface of a three-dimensional topological insulator. By using the diagrammatic expansion, we show that the coupling of an electron with the gauge field in the presence of impurity scatterings opens a gap around the Dirac node. The results are consistent with a recent experimental finding by Sato et al. [Nat. Phys. **7** (2011) 840]. We also discuss the consistency between the present results and the bulk-boundary correspondence of the topological insulator in the presence of time reversal symmetry. The conclusion can be applied to any two-dimensional massless fermions.

KEYWORDS: strong topological insulator, Dirac particle, gapped spectra, disorder, gauge field

1. Introduction

Properties of metallic states at the surface of topologically non-trivial materials are a hot issue in the condensed matter physics. A three-dimensional (3D) topological insulator (TI) hosts a metallic state with linear dispersion at its surface as a result of the topologically non-trivial nature of the wave function in bulk insulating region.¹⁻⁴⁾ Reflecting the shape of the dispersion, such metallic state is called Dirac cone. A point in the momentum space at which the upper cone and the lower one touch with each other is called Dirac node. The bulk-boundary correspondence suggests the presence of a single Dirac node at the surface, which reflects a topological number $Z_2 = 1$ in the bulk insulating region.

The presence of the single Dirac node is considered to be very robust against any perturbations preserving time reversal symmetry (TRS). To make clear the robustness of the Dirac node on the surface of 3DTI, we briefly mention the Dirac nodes on graphene for comparison. The graphene hosts the two distinct Dirac cones in the Brillouin zone. The Dirac nodes on graphene are protected by the sublattice and the chiral symmetries. Thus perturbations breaking these symmetries remove the Dirac nodes from graphene.^{5,6)} The sublattice symmetry enables the expression of the two-dimensional Dirac Hamiltonian $H = v(p_x s_x + p_y s_y)$ in which the momenta are coupled with so called pseudospin s_i with $i = x, y$, and z . Breaking the sublattice symmetry generates a mass term like $m s_z$ which removes the Dirac nodes.⁷⁻¹¹⁾ Due to the chiral symmetry, two Dirac cones have the opposite chirality to each other. The electron-electron interactions, for instance, mix the two Dirac cones and give rise to so called Dirac mass. As a consequence, graphene undergoes the metal-insulator phase transition.^{6,12-17)}

The Dirac node on the strong 3DTI, on the other hand, is protected only by TRS. Therefore possible mechanisms for the mass generation are very limited.¹⁸⁾ Since the momenta are coupled with real spin σ_i with $i = x, y$, and z , magnetic perturbations give a mass term like $m_z \sigma_z$, which is realized by magnetic moments¹⁹⁻²¹⁾ and magnetic impurities.²²⁻²⁵⁾ However such magnetic perturbations break TRS. According to the Nielsen-Ninomiya's theorem,²⁶⁾ the strong 3DTI also

hosts two Dirac cones with opposite chirality. However they are spatially separated each other when the sample of 3DTI is sufficiently thick. Namely when one Dirac cone stays at one surface, the other Dirac cone stays at the other surface. These Dirac cones can interact with each other only when the films of TI are sufficiently thin.²⁷⁻³³⁾ Therefore the Dirac node on strong 3DTI is very robust against perturbations which preserve TRS such as impurity scatterings and instantaneous electron-electron interactions.

A recent experiment,³⁴⁾ however, has reported the gapped excitation spectra in the single Dirac cone at the surface of $\text{TlBi}_2(\text{Se}_x\text{S}_{1-x})_3$. Starting with a topological insulator TlBi_2Se_3 , the gradual substitution of Selenium by Sulfur enables to make a series of insulators ended with a topologically trivial insulator TlBi_2S_3 . The insulators should be topological and should have a gapless single Dirac cone at their surface in the doping range of $0.5 < x \leq 1.0$. The experimental results of the angle resolved photo emission, however, clearly shows the gapped excitation spectra in the corresponding doping range. At present, we do not have any reasonable argument which explains the discrepancy between the theoretical prediction and the experimental results.

Motivated by the experiment,³⁴⁾ we theoretically try to make clear a mechanism which generates the gap around the Dirac node in the presence of the TRS. We consider the massless fermion in two-dimension which couples with the gauge field in the presence of normal impurity scatterings. The self-energy due to the impurity scatterings and the coupling with the gauge field is calculated within the lowest order of perturbation expansion. The results show that the real part of the self-energy for the upper Dirac cone has the opposite sign to that for the lower cone. As a result, two-dimensional fermion has gapped energy spectra around the Dirac node. We conclude that the interplay between the impurity scatterings and the coupling with the gauge field generates the gap. The results suggest the absence of gapless surface state even in the presence of TRS. We will show that our conclusion is not inconsistent with the bulk-boundary correspondence of TI's. We also conclude that the translational symmetry is necessary to preserve the gapless surface state in real TIs.

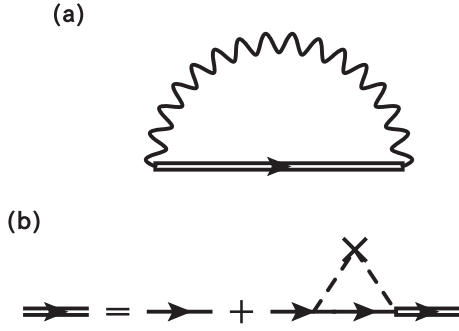


Fig. 1. The Feynman diagrams under consideration. (a) Fermion self-energy coupled to the gauge boson. The wavy line denotes the propagator of the gauge boson. (b) Dirac fermion propagator in the presence of impurity scatterings within the Born approximation.

This paper is organized as follows. In Sect. 2, we explain our theoretical model. The self-energy due to the coupling with the gauge field in the presence of the impurity scatterings is calculated in Sect. 3. We discuss a relation between theoretical results and an experimental one in Sect. 4. The conclusion is given in Sect. 5.

2. Theoretical Model

Let us consider the Lagrangian density which describes the two-dimensional massless Dirac fermions coupling with the gauge field,

$$\mathcal{L} = \sum_{j=0,1,2} \psi^\dagger (\tilde{p}_j - eA_j) \sigma^j \psi - \frac{1}{4} F_{\mu\nu} F^{\mu\nu}, \quad (1)$$

where σ^0 is the 2×2 unit matrix, σ^j for $j = 1-3$ are the Pauli matrices, ψ and A are the field operators of a surface massless fermion and a $U(1)$ gauge boson. In Eq. (1), $p_0 = \tilde{p}_0$ represents energy measured from the Dirac node and $p_j = \tilde{p}_j/v$ for $j = 1-2$ represents the momenta multiplied by the speed of light c where $v = v_F/c$ is a small constant describing dimensionless velocity with v_F being the Fermi velocity. Throughout this paper, we use the units of $\hbar = c = 1$. The field tensor $F^{\mu\nu}$ is defined by

$$F^{\mu\nu} = \partial^\mu A^\nu - \partial^\nu A^\mu, \quad (2)$$

with $\partial^\mu = \partial/\partial x_\mu$. We consider the Dirac propagator defined by

$$G_0(p) = \frac{p_0 \sigma^0 + v \mathbf{p} \cdot \boldsymbol{\sigma}}{p_0^2 - v^2 \mathbf{p}^2 + i\epsilon}, \quad (3)$$

where we take a short-hand notation $p = (p_0, \mathbf{p})$. Equation (3) represents the particle propagator for positive energy $p_0 > 0$ and the hole propagator for negative energy $p_0 < 0$. For the single gauge boson process as shown in Fig. 1(a) or 2(a), a two-dimensional Dirac particle interacts with a gauge boson having two-dimensional momentum. This is a natural consequence of the energy-momentum conservation law at each vertex according to the Feynman's rule. We employ the Feynman gauge in which the propagator converges at the spacial infinity $x_j \rightarrow \infty$ with $j = 1-2$. The propagator of the gauge field at energy q_0 and momentum \mathbf{q} is given by

$$D_{\mu\nu}(q) = \frac{-g_{\mu\nu}}{q_0^2 - \mathbf{q}^2 + i\epsilon}, \quad (4)$$

$$g_{\mu\nu} = \text{diag}\{1, -1, -1\}, \quad (5)$$

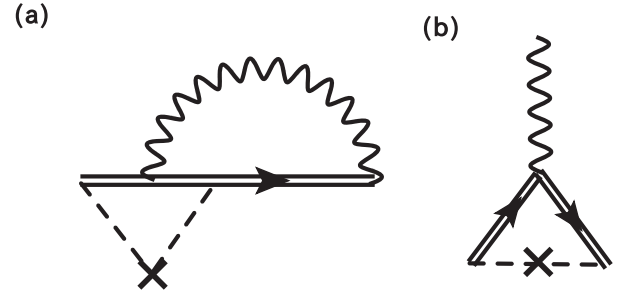


Fig. 2. The Feynman diagrams we consider in the text. (a) Fermion self-energy consisting of the gauge boson and the impurity scatterings. (b) Vertex function including the impurity scatterings.

where μ and ν are 0, 1, and 2. As shown in Eq. (1), the vertex of the coupling between the electron and the gauge field is described by $-e\sigma^\mu$ in Heaviside unit. We assume that the impurity potential is spin-independent and is represented by the delta-function,

$$U_i(\mathbf{r}) = \sum_j u \sigma^0 \delta(\mathbf{r} - \mathbf{r}_j), \quad (6)$$

where \mathbf{r}_j is the position of an impurity and u is the strength of a single impurity potential. We assume a constant density of impurities n_i .

3. Self-Energy

At first, we estimate the self-energy by the impurity scatterings alone. The impurity potential mixes the states with different momenta. It, however, does not mix the states with different energies. Therefore impurity scatterings itself cannot open the gap at the Dirac node. The self-energy within the Born approximation is represented by

$$\Sigma^{(i)} = -i\gamma p_0 \sigma^0, \quad (7)$$

where $\gamma = \pi u^2 n_i / v^2 > 0$ is the dimensionless expansion parameter smaller than unity (see also Appendix A). The result has the general form of the massless Dirac fermion.³⁵⁾

Secondly, we calculate the self-energy of a Dirac fermion coupled with the gauge field which is given by

$$\Sigma^{(g)}(p) = \sum_q \sum_{\mu\nu} (-e\sigma^\mu) G_0(p-q) (-e\sigma^\nu) D_{\mu\nu}(q). \quad (8)$$

The details of calculation are shown in Appendix B, where we estimate the self-energy in Fig. 1(a). Namely we calculate $\Sigma^{(g)}(p)$ in Eq. (8) with using the full Green function $G(p-q)$ in Eq. (B.1) instead of the bare $G_0(p-q)$ in Eq. (3). In the limit of small momenta, the real part of the self-energy has an asymptotic form as

$$\text{Re}[\Sigma^{(g)}(p)] = \pi e^2 \left(\frac{p_0 \sigma^0}{\sqrt{p_0^2}} - \frac{\mathbf{p} \cdot \boldsymbol{\sigma}}{\sqrt{\mathbf{p}^2}} \right). \quad (9)$$

We note that the result does not contain γ . Therefore the impurity scatterings add only negligible corrections to Eq. (9) as shown in Appendix B. From pole of the scalar denominator $[G_0(p)^{-1} - \Sigma^{(g)}(p)]$, this self energy cannot open gap for massless Dirac fermion,

$$\begin{aligned} p_0 &= \pm(v|\mathbf{p}| + \pi e^2) - \pi e^2 \text{sgn}(p_0) \\ &= \pm v|\mathbf{p}|. \end{aligned} \quad (10)$$

The two terms stemming from the self-energy cancel each other out, which reflects the covariance of the gauge field. As a consequence, the coupling with the gauge field does not change the energy spectra of massless Dirac fermion.

Neither the coupling with gauge field alone nor the impurity scatterings alone open the gap at the Dirac node. The former changes the energy of a fermion but preserves the translational symmetry. The latter breaks the translational symmetry but preserves the energy of fermion. To have a gap at the Dirac node, we need scattering processes which change the momenta due to breaking the translational symmetry and the energy of a fermion at the same time.

Finally, we consider a self-energy which represents the interplay between the coupling with the gauge field and the impurity scatterings. The scattering processes are diagrammatically described in Fig. 2(a). Such self-energy is given by

$$\Sigma(p) = \sum_{p_0, q, \mu, \nu} \Gamma^\mu(p_0', q) G(p - q) (-e\sigma^\nu) D_{\mu, \nu}(q), \quad (11)$$

$$\Gamma^\mu(p_0, q) = \gamma \sum_p G(p) (-e\sigma^\mu) G(p - q), \quad (12)$$

where $\Gamma_\mu(p_0, q)$ is the vertex function shown in Fig. 2(b). The vertex function can be derived from the Ward–Takahashi’s identity^{36,37} with the self-energy of impurity scatterings in Eq. (7),

$$\begin{aligned} (p' - p)^\mu (\sigma_\mu + \Gamma_\mu(p, p')) \\ = p' - \Sigma^{(i)}(p') - (p - \Sigma^{(i)}(p)). \end{aligned} \quad (13)$$

The vertex function results in

$$\Gamma^\mu(p, p') = -ie\gamma\delta^{0\mu}, \quad (14)$$

where $\delta^{\mu\nu}$ is the Kronecker’s delta. The correction at another vertex of gauge field [Fig. 2(a)] give the same contribution. Thus the self-energy in Eq. (11) becomes

$$\Sigma(p) = 2i\gamma e^2 \sum_q G(p - q) \frac{1}{q_0^2 - \mathbf{q}^2 + i\epsilon}. \quad (15)$$

The summation of q can be done using the method for deriving Eq. (8). By introducing a parameter $x_0 = v^2 \mathbf{p}^2 / p_0^2$, we obtain the expression of the self-energy in the limit of $x_0 \rightarrow 0$ as

$$\lim_{p \rightarrow 0} \Sigma(p_0, \mathbf{p}) = 2\pi e^2 \gamma^2 ((\text{sgn}(p_0)\sigma^0 + \hat{\mathbf{p}} \cdot \boldsymbol{\sigma}), \quad (16)$$

where $\hat{\mathbf{p}}$ is the unit vector in the direction of \mathbf{p} . This is the central result of this paper. The result does not depend on either the magnitude of the energy or that of the momentum. From the pole of the scalar denominator of $[G_0(p)^{-1} - \Sigma(p)]$, we obtain the energy dispersion of perturbed fermions at $|\mathbf{p}| \rightarrow 0$ as

$$\begin{aligned} p_0 &= \pm(v|\mathbf{p}| + 2\pi e^2 \gamma^2) + 2\pi e^2 \gamma^2 \text{sgn}(p_0) \\ &= \pm(v|\mathbf{p}| + 4\pi e^2 \gamma^2). \end{aligned} \quad (17)$$

The result shows the gapped energy spectra around the Dirac node. We note that both the impurity scatterings and the coupling to the gauge field preserve the TRS.

4. Discussion

According to the features of the spectra in Eq. (17), the

magnitude of the gap should be independent of temperature. Our results are consistent with the gapped spectra found in the experiment by Sato et al.³⁴ Another experiment³⁸ has reported the gapless spectra in the similar situation. The energy resolution of experiment in Ref. 34 seems to be better than that in Ref. 38.

We discuss effects of electron–electron interactions via the gauge field on the excitation spectra around the Dirac node. Because of the dynamics of the gauge field, the interaction potential depends on frequency. As a result, the interplay between the impurity scatterings and the interaction via the gauge field opens the gap at the Dirac node. On the other hand, in condensed matter physics, the electron–electron interactions are usually taken into account within the static approximation. Namely, the Coulomb interaction acts two fermions at an equal time. Therefore such static interactions do not depend on the frequency. The two different types of interactions in the presence of impurity scatterings may affect the excitation spectra in two different ways. In one-dimension, sufficiently strong static interactions cause the gap.³⁹ In two-dimension, however, the excitation spectra have been believed to remain gapless even in the strong static interactions. On the other hand, we show that the electron–electron interactions via the dynamical boson field lead to qualitatively different results of the gapped spectra in two-dimension. In fact, the results in Eq. (17) are obtained within the lowest order of $v = v_F/c \ll 1$. This argument is also important when we consider topological protection of the gapless surface state by the bulk-boundary correspondence, which we discuss next.

Finally, it is necessary to discuss a relationship between our results and the bulk-boundary correspondence of three-dimensional TI in the presence of the TRS. The Z_2 invariant is well defined in (1 + 3) dimensional fermion space of TI.¹ The bulk-boundary correspondence works well to understand the existence of the two-dimensional gapless state on its surface. In this paper, however, we consider a situation in which the fermion on TI naturally couples with the electromagnetic field. In such situation, the whole physical space consists of the fermion space and the gauge boson one. Namely, the (1 + 3) dimensional fermion space is no longer closed independent physical space. At present, it is unclear if it is possible to apply the topological classification defined solely in the fermion space to the integrated physical space of the fermion and the gauge boson. Even in the integrated space, it may be still possible to consider the topological characterization in the fermion space only. In such case, the theory would be possible to define some topological invariants in a similar way as the weak topological invariants.⁴⁰ Therefore the predictions by the topological theory^{1-3,41,42} in (1 + 3) dimensional fermion space are not always valid. This makes the background of the gapped energy spectra appearing at the topologically protected surface state. The coupling of fermion with another degree of freedom sometimes changes a topologically non-trivial phase to a topologically trivial one. Our result demonstrates an example of the story.

5. Conclusion

In conclusion, we have studied effects of the gauge field

and the impurity scatterings on the energy spectra of massless Dirac fermion at the surface of a three-dimensional topological insulator. By using the perturbation expansion, we have calculated the self-energy around the Dirac node. The interplay between the impurity scatterings and the coupling with the gauge field leads to the gapped energy dispersion around the Dirac node.

Acknowledgments

This work was supported by the ‘‘Topological Quantum Phenomena’’ (No. 22103002) Grant-in-Aid for Scientific Research on Innovative Areas from the Ministry of Education, Culture, Sports, Science and Technology of Japan (MEXT).

Appendix A: Self-Energy due to Impurity Scatterings

We derive the self-energy of impurity scattering alone. Within the Born approximation, the self-energy is given by,

$$\Sigma^{(i)} = u^2 n_i \int d^2\mathbf{p} \frac{p_0 \sigma^0 + \mathbf{v}\mathbf{p} \cdot \boldsymbol{\sigma}}{p_0^2 - v^2 \mathbf{p}^2 + i\varepsilon}. \quad (\text{A}\cdot 1)$$

The term proportional to momentum \mathbf{p} vanishes after integrating of \mathbf{p} . The self-energy is calculated as

$$\Sigma^{(g)}(p) = \sum_q \sum_{\mu\nu} (-e\sigma^\mu) G(p-q) (-e\sigma_\nu) D_{\mu\nu}(q) \quad (\text{B}\cdot 2)$$

$$= \sum_{q_0, \mathbf{q}} \sum_{\mu\nu} (-e\sigma_\mu) \frac{(1+i\gamma)(p_0 - q_0)\sigma^0 + \mathbf{v}(\mathbf{p} - \mathbf{q}) \cdot \boldsymbol{\sigma}}{(1+i\gamma)^2(p_0 - q_0)^2 - v^2(\mathbf{p} - \mathbf{q})^2} (-e\sigma_\nu) \frac{-g_{\mu\nu}}{q_0^2 - \mathbf{q}^2 + i\varepsilon}. \quad (\text{B}\cdot 3)$$

The self-energy is expressed in the parametric integral representation⁴³⁾ as,

$$\Sigma^{(g)}(p) = g_{\mu\nu} \lim_{x \rightarrow 0} \int_{-\infty}^{\infty} \frac{dq_0 d^2\mathbf{q}}{(\sqrt{2\pi})^3} \int_0^{\infty} \int_0^{\infty} d\alpha_1 d\alpha_2 (-e\sigma^\mu) \frac{1}{i} (\sigma_0 \partial_{x_0} - \boldsymbol{\sigma} \cdot \boldsymbol{\partial}_x) (-e\sigma^\nu) \exp(iS), \quad (\text{B}\cdot 4)$$

$$S = \alpha_1((1+i\gamma)^2(p_0 - q_0)^2 - v_F^2(\mathbf{p} - \mathbf{q})^2 + i\varepsilon) + \alpha_2(q_0^2 - \mathbf{q}^2 + i\varepsilon) + x_0(1+i\gamma)(p_0 - q_0) - \mathbf{v}\mathbf{x} \cdot (\mathbf{p} - \mathbf{q}), \quad (\text{B}\cdot 5)$$

where x_μ and α_j are dummy variables. The integral with respect to the momenta can be done by the Fresnel integral. The results become

$$\Sigma^{(g)}(p) = -e^2 \lim_{x \rightarrow 0} \int_0^{\infty} \int_0^{\infty} \frac{d\alpha_1 d\alpha_2}{(\alpha_1 v^2 + \alpha_2) \sqrt{i(\alpha_1(1+i\gamma)^2 + \alpha_2)}} \frac{1}{i} (\sigma_0 \partial_{x_0} + \boldsymbol{\sigma} \cdot \boldsymbol{\partial}_x) \times \exp \left[i \left\{ (\alpha_1 + \alpha_2)\varepsilon + \frac{\alpha_1 \alpha_2 (1+i\gamma) p_0^2}{\alpha_1(1+i\gamma) + \alpha_2} - \frac{\alpha_1 \alpha_2 \mathbf{p}^2}{\alpha_1 v^2 + \alpha_2} - \frac{\alpha_2 (1+i\gamma) p_0 x_0}{\alpha_1(1+i\gamma)^2 + \alpha_2} + \frac{\mathbf{v}\mathbf{x} \cdot \mathbf{p}}{\alpha_1 v^2 + \alpha_2} \right\} \right].$$

Next we introduce a integration variable $\rho = \alpha_1 + \alpha_2$ and change the integration variables as $\alpha_i \rightarrow \rho\alpha_i$. In this way, we obtain

$$\Sigma^{(g)}(p) = -e^2 \int_0^1 \int_0^1 \frac{d\alpha_1 d\alpha_2}{\alpha_1 v^2 + \alpha_2} \frac{\delta(1 - \alpha_1 - \alpha_2)}{\sqrt{i(\alpha_1(1+i\gamma)^2 + \alpha_2)}} \left(\frac{\alpha_2(1+i\gamma)}{\alpha_1(1+i\gamma)^2 + \alpha_2} p_0 \sigma^0 - \frac{\alpha_2}{\alpha_1 v^2 + \alpha_2} \mathbf{v}\mathbf{p} \cdot \boldsymbol{\sigma} \right) \times \int_0^{\infty} \frac{d\rho}{\sqrt{i\rho}} \exp \left[-\rho \left(\varepsilon + \frac{\alpha_1 \alpha_2 (1+i\gamma)^2}{i(\alpha_1(1+i\gamma)^2 + \alpha_2)} p_0^2 - \frac{\alpha_1 \alpha_2}{i(\alpha_1 v^2 + \alpha_2)} v^2 \mathbf{p}^2 \right) \right]. \quad (\text{B}\cdot 6)$$

By applying the condition $v^2 \ll 1$ and introducing a variable $x_0 = v^2 \mathbf{p}^2 / p_0^2$, the self-energy becomes

$$\Sigma^{(g)}(p) \simeq -e^2 \int_0^1 \frac{d\alpha}{\sqrt{\alpha((1+i\gamma)^2 p_0^2 (1-\alpha) - (1+(2i\gamma + \gamma^2)\alpha)v^2 \mathbf{p}^2)}} \left(\frac{1+i\gamma}{1+2i\gamma\alpha} p_0 \sigma^0 - \frac{\mathbf{v}\mathbf{p} \cdot \boldsymbol{\sigma}}{1-\alpha} \right) \quad (\text{B}\cdot 7)$$

$$\simeq -\frac{e^2}{\sqrt{p_0^2}} (1-i\gamma) \int_0^1 \frac{d\alpha}{\sqrt{\alpha((1-x_0) - \alpha)}} \left(1 + \frac{\gamma(2i+\gamma)}{2(1+i\gamma)^2} \frac{1-\alpha}{1-\alpha-x_0} x_0 \right) \left(\frac{1+i\gamma}{1+2i\gamma\alpha} p_0 \sigma^0 - \frac{\mathbf{v}\mathbf{p} \cdot \boldsymbol{\sigma}}{1-\alpha} \right). \quad (\text{B}\cdot 8)$$

We neglect terms proportional to x_0 because we focus on the limit of $x_0 \simeq 0$ in the followings. The results are

$$\Sigma^{(g)}(p) \simeq -\frac{e^2}{\sqrt{p_0^2}} \left(\int_{1-x_0}^1 \frac{d\alpha}{i\sqrt{\alpha(\alpha - (1-x_0))}} + \int_0^{1-x_0} \frac{d\alpha}{\sqrt{\alpha((1-x_0) - \alpha)}} \right) \left((1+i\gamma - 2i\gamma\alpha) p_0 \sigma^0 - \frac{\mathbf{v}\mathbf{p} \cdot \boldsymbol{\sigma}}{1-\alpha} \right) \quad (\text{B}\cdot 9)$$

$$= -\frac{e^2}{\sqrt{p_0^2}} (1-i\gamma) \left(-i(1+i\gamma) p_0 \sigma^0 [\log(2\alpha - (1-x_0) + 2\sqrt{\alpha(\alpha - (1-x_0))})] \Big|_{1-x_0} \right)$$

$$\Sigma^{(i)} = u^2 n_i \int \frac{d^2\mathbf{p}}{(\sqrt{2\pi})^2} \frac{p_0 \sigma^0}{p_0^2 - v^2 \mathbf{p}^2 + i\varepsilon} = u^2 n_i p_0 \sigma^0 \times \int \frac{d^2\mathbf{p}}{(\sqrt{2\pi})^2} \int_0^{\infty} \frac{d\alpha}{(-i)} \exp[i\alpha(p_0^2 - v^2 \mathbf{p}^2 + i\varepsilon)] = -i\gamma p_0 \sigma^0, \quad (\text{A}\cdot 2)$$

$$\gamma = \pi u^2 n_i / v^2. \quad (\text{A}\cdot 3)$$

The resulting self-energy is pure imaginary and gives the inverse of the life time in agreement with a previous result.³⁵⁾ We introduce a dimensionless constant γ which contains material parameters.

Appendix B: Self-Energy due to Coupling with Gauge Field

Let us calculate the self-energy due to coupling with the gauge field represented by Fig. 1(a). The propagator for a Dirac fermion in the presence of impurity scattering is represented by

$$G(p) = \frac{(1+i\gamma)p_0 \sigma^0 + \mathbf{v}\mathbf{p} \cdot \boldsymbol{\sigma}}{(1+i\gamma)^2 p_0^2 - v^2 \mathbf{p}^2}. \quad (\text{B}\cdot 1)$$

By using this propagator, the self-energy in Fig. 1(a) is given by

$$\begin{aligned}
 & - (1 + i\gamma)p_0\sigma^0 \left[\arcsin \frac{-2\alpha + (1 - x_0)}{1 - x_0} \right]_0^{1-x_0} \\
 & - 2\gamma p_0\sigma^0 \left[\sqrt{\alpha(\alpha - (1 - x_0))} - (1 - x_0) \log \left| \frac{\sqrt{\alpha - (1 - x_0)} - \sqrt{\alpha}}{\sqrt{\alpha - (1 - x_0)} + \sqrt{\alpha}} \right| \right]_{1-x_0}^1 \\
 & - 2i\gamma p_0\sigma^0 \left[\sqrt{\alpha((1 - x_0) - \alpha)} - (1 - x_0) \arcsin \sqrt{\frac{(1 - x_0) - \alpha}{1 - x_0}} \right]_0^{1-x_0} \\
 & + i \frac{v\mathbf{p} \cdot \boldsymbol{\sigma}}{\sqrt{x_0}} \left[\log \frac{(2\alpha - (1 - x_0))(\alpha - 1) + 2x_0 - 2\sqrt{x_0\alpha(\alpha - (1 - x_0))}}{\alpha - 1} \right]_{1-x_0}^1 \\
 & - \frac{v\mathbf{p} \cdot \boldsymbol{\sigma}}{\sqrt{x_0}} \left[\arcsin \frac{(-1 - x_0)(1 - \alpha) + 2x_0}{(1 - x_0)(1 - \alpha)} \right]_0^{1-x_0} \Big). \tag{B-10}
 \end{aligned}$$

We reach the self-energy as

$$\begin{aligned}
 \Sigma^{(g)}(p) \simeq & - \frac{e^2}{\sqrt{p_0^2}} (1 - i\gamma) \left(-i(1 + i\gamma)p_0\sigma^0 \log \frac{1 + x_0 + 2\sqrt{x_0}}{1 - x_0} + \pi p_0\sigma^0 - 2\gamma p_0\sigma^0 \sqrt{x_0} \right. \\
 & \left. + 2\gamma p_0\sigma^0 (1 - x_0) \log \frac{1 - \sqrt{x_0}}{1 + \sqrt{x_0}} + i\pi\gamma p_0\sigma_0 x_0 - i \frac{v\mathbf{p} \cdot \boldsymbol{\sigma}}{\sqrt{x_0}} \log(1 + x_0) - \pi \frac{v\mathbf{p} \cdot \boldsymbol{\sigma}}{\sqrt{x_0}} \right). \tag{B-11}
 \end{aligned}$$

Using $x_0 = v^2 p^2 / p_0^2 \ll 1$, it becomes

$$\begin{aligned}
 \Sigma^{(g)}(p) \simeq & -e^2 (1 - i\gamma) \left(\pi \frac{p_0\sigma^0}{\sqrt{p_0^2}} - \pi \frac{\mathbf{p} \cdot \boldsymbol{\sigma}}{\sqrt{p^2}} - 2\gamma \sqrt{x_0} \frac{p_0\sigma^0}{\sqrt{p_0^2}} + 2\gamma (1 - x_0) \log \left(\frac{1 - \sqrt{x_0}}{1 + \sqrt{x_0}} \right) \frac{p_0\sigma^0}{\sqrt{p_0^2}} \right. \\
 & \left. - i(1 + i\gamma) \frac{p_0\sigma^0}{\sqrt{p_0^2}} \log \frac{1 + x_0 + 2\sqrt{x_0}}{1 - x_0} + i\pi\gamma x_0 \frac{p_0\sigma^0}{\sqrt{p_0^2}} - i \log(1 + x_0) \frac{\mathbf{p} \cdot \boldsymbol{\sigma}}{\sqrt{p^2}} \right). \tag{B-12}
 \end{aligned}$$

Finally by putting $\gamma \rightarrow 0$, it is possible to obtain the self-energy due to the gauge field alone.

*ha-bet@eng.hokudai.ac.jp

- 1) L. Fu, C. L. Kane, and E. J. Mele: *Phys. Rev. Lett.* **98** (2007) 106803.
- 2) L. Fu and C. L. Kane: *Phys. Rev. B* **76** (2007) 045302.
- 3) J. E. Moore and L. Balents: *Phys. Rev. B* **75** (2007) 121306.
- 4) Y. L. Chen, J. G. Analytis, J.-H. Chu, Z. K. Liu, S. K. Mo, X. L. Qi, H. J. Zhang, D. H. Lu, X. Dai, Z. Fang, S. C. Zhang, I. R. Fisher, Z. Hussain, and Z. X. Shen: *Science* **325** (2009) 178.
- 5) A. H. Castro Neto, F. Guinea, N. M. R. Peres, K. S. Novoselov, and A. K. Geim: *Rev. Mod. Phys.* **81** (2009) 109.
- 6) V. N. Kotov, B. Uchoa, V. M. Pereira, F. Guinea, and A. H. Castro Neto: *Rev. Mod. Phys.* **84** (2012) 1067.
- 7) S. Y. Zhou, G.-H. Gweon, A. V. Fedorov, P. N. First, W. A. de Heer, D.-H. Lee, F. Guinea, A. H. C. Neto, and A. Lanzara: *Nat. Mater.* **6** (2007) 770.
- 8) K. Novoselov: *Nat. Mater.* **6** (2007) 720.
- 9) G. Giovannetti, P. A. Khomyakov, G. Brocks, P. J. Kelly, and J. van den Brink: *Phys. Rev. B* **76** (2007) 073103.
- 10) S. Kim, J. Ihm, H. J. Choi, and Y.-W. Son: *Phys. Rev. Lett.* **100** (2008) 176802.
- 11) R. Balog, B. Jorgensen, L. Nilsson, M. Andersen, E. Rienks, M. Bianchi, M. Fanetti, E. Lgsgaard, A. Baraldi, S. Lizzit, Z. Sljivancanin, F. Besenbacher, B. Hammer, T. G. Pedersen, P. Hofmann, and L. Hornekr: *Nat. Mater.* **9** (2010) 315.
- 12) E. V. Gorbar, V. P. Gusynin, V. A. Miransky, and I. A. Shovkovy: *Phys. Rev. B* **66** (2002) 045108.
- 13) D. Khveshchenko and H. Leal: *Nucl. Phys. B* **687** (2004) 323.
- 14) D. Khveshchenko: *J. Phys.: Condens. Matter* **21** (2009) 075303.
- 15) G.-Z. Liu, W. Li, and G. Cheng: *Phys. Rev. B* **79** (2009) 205429.
- 16) O. V. Gamayun, E. V. Gorbar, and V. P. Gusynin: *Phys. Rev. B* **80** (2009) 165429.
- 17) O. V. Gamayun, E. V. Gorbar, and V. P. Gusynin: *Phys. Rev. B* **81** (2010) 075429.
- 18) M. Z. Hasan and C. L. Kane: *Rev. Mod. Phys.* **82** (2010) 3045.
- 19) Y. Tanaka, T. Yokoyama, and N. Nagaosa: *Phys. Rev. Lett.* **103** (2009) 107002.
- 20) L. A. Wray, S.-Y. Xu, Y. Xia, D. Hsieh, A. V. Fedorov, Y. S. Hor, R. J. Cava, A. Bansil, H. Lin, and M. Z. Hasan: *Nat. Phys.* **7** (2011) 32.
- 21) T. Haba and Y. Asano: *Phys. Rev. B* **85** (2012) 195325.
- 22) D. Hsieh, Y. Xia, D. Qian, L. Wray, J. H. Dil, F. Meier, J. Osterwalder, L. P. J. G. Checkelsky, N. P. Ong, A. V. Fedorov, H. Lin, A. Bansil, D. Grauer, Y. S. Hor, R. J. Cava, and M. Z. Hasan: *Nature* **460** (2009) 1101.
- 23) Q. Liu, C.-X. Liu, C. Xu, X.-L. Qi, and S.-C. Zhang: *Phys. Rev. Lett.* **102** (2009) 156603.
- 24) Y. S. Hor, P. Roushan, H. Beidenkopf, J. Seo, D. Qu, J. G. Checkelsky, L. A. Wray, D. Hsieh, Y. Xia, S.-Y. Xu, D. Qian, M. Z. Hasan, N. P. Ong, A. Yazdani, and R. J. Cava: *Phys. Rev. B* **81** (2010) 195203.
- 25) Y. L. Chen, J.-H. Chu, J. G. Analytis, Z. K. Liu, K. Igarashi, H.-H. Kuo, X. L. Qi, S. K. Mo, R. G. Moore, D. H. Lu, M. Hashimoto, T. Sasagawa, S. C. Zhang, I. R. Fisher, Z. Hussain, and Z. X. Shen: *Science* **329** (2010) 659.
- 26) H. B. Nielsen and M. Ninomiya: *Phys. Lett. B* **130** (1983) 389.
- 27) B. Seradjeh, J. E. Moore, and M. Franz: *Phys. Rev. Lett.* **103** (2009) 066402.
- 28) J. Wang, A. M. DaSilva, C.-Z. Chang, K. He, J. K. Jain, N. Samarth, X.-C. Ma, Q.-K. Xue, and M. H. W. Chan: *Phys. Rev. B* **83** (2011) 245438.
- 29) M. Liu, C.-Z. Chang, Z. Zhang, Y. Zhang, W. Ruan, K. He, L.-I. Wang, X. Chen, J.-F. Jia, S.-C. Zhang, Q.-K. Xue, X. Ma, and Y. Wang: *Phys. Rev. B* **83** (2011) 165440.
- 30) G. Y. Cho and J. E. Moore: *Phys. Rev. B* **84** (2011) 165101.
- 31) E. G. Moon and C. Xu: *Europhys. Lett.* **97** (2012) 66008.
- 32) I. Sodemann, D. A. Pesin, and A. H. MacDonald: *Phys. Rev. B* **85** (2012) 195136.
- 33) D. K. Efimkin, Y. E. Lozovik, and A. A. Sokolik: *Phys. Rev. B* **86** (2012) 115436.
- 34) T. Sato, K. Segawa, K. Kosaka, S. Souma, K. Nakayama, K. Eto, T. Minami, Y. Ando, and T. Takahashi: *Nat. Phys.* **7** (2011) 840.
- 35) H. Suzuura and T. Ando: *Phys. Rev. Lett.* **89** (2002) 266603.
- 36) J. C. Ward: *Phys. Rev.* **78** (1950) 182.
- 37) Y. Takahashi: *Nuovo Cimento* **6** (1957) 371.
- 38) S.-Y. Xu, Y. Xia, L. A. Wray, S. Jia, F. Meier, J. H. Dil, J. Osterwalder, B. Slomski, A. Bansil, H. Lin, R. J. Cava, and M. Z. Hasan: *Science* **332** (2011) 560.
- 39) C. Xu and J. E. Moore: *Phys. Rev. B* **73** (2006) 045322.
- 40) R. Roy: *Phys. Rev. B* **79** (2009) 195322.
- 41) R. Roy: *arXiv:1004.3507*.
- 42) X.-L. Qi, T. L. Hughes, and S.-C. Zhang: *Phys. Rev. B* **78** (2008) 195424.
- 43) M. C. Bergère and J. B. Zuber: *Commun. Math. Phys.* **35** (1974) 113.